OPTIMIZATION OF CAPACITIVE CURRENT CALCULATION FOR 10 kV DISTRIBUTION NETWORK BASED ON GA-PSO-MCS

Jie BAI[1], Jianzhong YANG[2], Lei WANG[3*], Bingjie DOU[4], Chun MIAO[5], Huiyang ZHANG[6]

To address the overestimation and uncertainty issues in traditional capacitive current calculation for Hohhot's 10kV grid, this paper proposes a hybrid GA-PSO-MCS optimization method. It automatically optimizes model parameters by minimizing the standard deviation of Monte Carlo Simulation results. Compared to conventional methods, this approach significantly reduces the estimated current to 95.56A, mitigating overestimation. Against other optimizers like PSO-MCS, it maintains accuracy while achieving a lower standard deviation (1.32A) and a higher confidence limit (98.31A), demonstrating reduced uncertainty and enhanced robustness for reliable arc suppression coil selection.

Keywords: Capacitive Current calculation; Distribution network; Hybrid optimization Algorithm; GA-PSO-MCS; Parameter optimization; Arc suppression coil

1. Introduction

Medium-voltage distribution networks, serving as a critical link between the transmission grid and end-users, play a vital role in ensuring the safety and reliability of power system operation. Among various fault types, distribution networks are susceptible to various faults, with the single-phase-to-ground (SPTG) fault [1] deserving particular attention due to its high frequency of occurrence. When such a fault occurs, the voltage of the non-faulted phases rises, resulting in a

[1] Inner Mongolia Power (Group) Co., Ltd, China; Inner Mongolia Power Research Institute, Hohhot 010020, China
[2] Inner Mongolia Power (Group) Co., Ltd, China; Inner Mongolia Power Research Institute, Hohhot 010020, China
[3] * Inner Mongolia Power (Group) Co., Ltd, China; Inner Mongolia Power Research Institute, Hohhot 010020, China, corresponding author, e-mail: nandanvt66@163.com
[4] Inner Mongolia Power (Group) Co., Ltd, China; Inner Mongolia Power Research Institute, Hohhot 010020, China
[5] Inner Mongolia Power (Group) Co., Ltd, China; Inner Mongolia Power Research Institute, Hohhot 010020, China
[6] Inner Mongolia Power (Group) Co., Ltd, China; Inner Mongolia Power Research Institute, Hohhot 010020, China

capacitive current flowing through the phase-to-ground (PTG) capacitance. If this capacitive current becomes excessively large, it can lead to an intermittent arc at the fault point, which may generate arcing overvoltage and even develop into a phase-to-phase short circuit, posing serious threats to grid equipment and personal safety. In China, the 10 kV voltage level has become the mainstream framework of urban and rural distribution networks due to its techno-economic advantages. With rapid urbanization and the continuous improvement of distribution network automation, the structure of 10 kV grids has become increasingly complex. The dual drivers of urbanization and distribution network automation present a significant challenge to the management of 10 kV grids, whose structures are evolving in complexity. The proportion of cable lines has significantly increased, and overhead lines are now commonly insulated. These developments have collectively led to a substantial increase in the system's PTG capacitance. Distribution systems generally adopt a non-effectively grounded neutral [2]. When a single-phase ground fault occurs in such systems, the fault current [3] is primarily composed of the capacitive current to ground, the magnitude of which depends on the total distributed PTG capacitance of all lines in the system. Accurate calculation and analysis of the capacitive current can effectively predict and prevent failures caused by excessive or unbalanced capacitive currents, such as single-phase ground overvoltage and arc-induced fires, thereby reducing the grid failure rate, ensuring power supply continuity and stability, and minimizing social and economic losses due to power interruptions [4]. Therefore, obtaining an accurate value of the system's PTG capacitive current is essential for analyzing and assessing the operational status of the power system.

Traditional methods for calculating the capacitive current in distribution networks primarily rely on deterministic models [5]. These models typically obtain empirical values of capacitive current per unit length from equipment manuals, perform a weighted summation based on line lengths, and add a fixed additional ratio to account for substation capacitance contribution. However, this approach exhibits significant limitations [6]: the actual types of lines are highly diverse, and using a single empirical value introduces considerable deviation. Furthermore, public lines and dedicated lines differ in operating environment, insulation aging, and other factors. Applying identical weight coefficients fails to accurately reflect their actual differences in unit capacitive current.

To overcome the shortcomings of traditional methods, researchers have gradually introduced various optimization algorithms and probabilistic analysis techniques. These methods exhibit distinct complementary characteristics throughout their evolution. The GA [7], widely applied in early stages, possesses strong global search capabilities but suffers from slow convergence rates. To improve convergence efficiency, the PSO algorithm [8]is proposed. Despite its simple structure and rapid convergence, PSO is susceptible to premature

convergence, often becoming trapped in local optima when optimizing complex multimodal functions. Bayesian Optimization (BO) [9] has garnered attention due to its high sample efficiency. It models the objective function using surrogate models like Gaussian Processes, effectively reducing the number of required evaluations. However, its performance is highly dependent on the setting of the prior distribution, and its computational complexity increases significantly in high-dimensional spaces. Evidently, each algorithm possesses inherent applicable scenarios and limitations.

Nevertheless, within the field of capacitive current calculation, existing research often employs a single method in isolation or separates the optimization process from uncertainty assessment. A systematic hybrid inference framework has not yet been established, thereby limiting further improvements in computational accuracy and practicality.

Addressing the above problems and limitations, this paper proposes a hybrid GA-PSO-MCS algorithm to enhance the calculation accuracy and reliability of capacitive current in 10kV distribution networks. The main contributions and innovations are as follows:

(1) A hybrid GA-PSO optimization strategy is designed, which involves alternately executing genetic operations (selection, crossover, mutation) and particle swarm iterations. This strategy synergistically optimizes key parameters such as public/dedicated line weights and the substation additional ratio to prevent premature convergence and converge more rapidly to the global optimal solution.

(2) The optimized parameters are embedded within a Monte Carlo simulation framework. Through 5000 random samplings, input parameters such as unit current values and line weights are treated as probability distributions. This process ultimately outputs the probability distribution of the capacitive current and its confidence interval at a specified confidence level, providing a probabilistic basis for the selection of arc suppression coils.

2. Fundamental principles

2.1 Distribution network capacitive current calculation

Utilizing a small-current grounding configuration in the distribution network [10], the single-phase grounding capacitive current primarily consists of two components: first, the PTG capacitive current from power lines such as cables and overhead lines; second, the PTG capacitive current originating from power equipment including synchronous generators, large-capacity synchronous motors, and transformers. Additionally, the capacitive contribution from absorption capacitors used for overvoltage protection in rotating machinery, as well as the capacitive component of RC absorption circuits employed to suppress switching

over-voltages in high-voltage vacuum circuit breakers, should also be taken into account.

Generally, the PTG capacitive current per unit length of overhead lines is significantly smaller than that of cable circuits. Moreover, the capacitive current generated by power equipment is an order of magnitude smaller than that produced by power lines. Therefore, in practical engineering calculations, the capacitive current from both cables and overhead lines is typically considered as the primary component. However, if synchronous generators or large-capacity synchronous motors [11] are connected to the system, their capacitive current cannot be neglected. In summary, a comprehensive calculation of the system's single-phase grounding capacitive current should include the sum of the capacitive currents from cables and overhead lines, as well as the PTG capacitive current from electrical equipment.

Based on the above theoretical foundation, take as an example a single-phase grounding fault occurring [12] in a 10kV distribution network (without an arc suppression coil). Its structure is shown in Fig. 1:

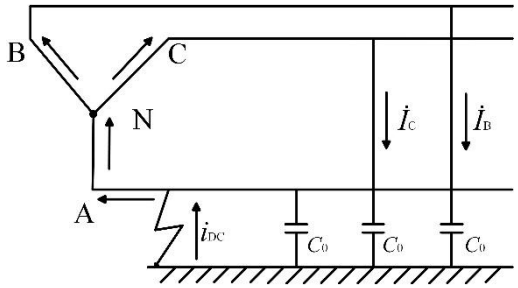

Fig. 1. Structure of a small-current grounding system under a STG fault.

When a single-phase ground fault occurs on phase A, a complete circuit is formed for phases B and C through the fault point, the PTG capacitances of the lines, and the earth. This results in a displacement of the neutral point, which shifts from its original position (point N) to the location of the fault. The fault current generated under this condition is as follows:

$$\dot{I}_{DC} = \dot{I}_B + \dot{I}_C \tag{1}$$

Upon the occurrence of a single-phase ground fault in an ungrounded system, the magnitude of the non-faulted phase voltages (phases B and C) increases to $\sqrt{3}$ times the original phase voltage. Therefore:

$$\dot{I}_B = \sqrt{3}\omega C_0 \dot{U}_B \tag{2}$$

$$\dot{I}_C = \sqrt{3}\omega C_0 \dot{U}_C \tag{3}$$

$$\dot{I}_{DC} = 3j\omega C_0 \dot{U}_N \tag{4}$$

The capacitive current from phase A to ground under pre-fault conditions is:

$$\dot{I}_A = j\omega C_0 \dot{U}_A \tag{5}$$

Therefore, when a SPTG fault occurs on phase A, the capacitive current flowing through the faulted phase increases to three times the PTG capacitive current under normal operating conditions.

As indicated by the equation, the magnitude of the system's single-phase grounding capacitive current is related to factors such as the grid voltage level, the PTG capacitance of the lines, and the system frequency. Under the specific conditions of this project, both the voltage level and the system frequency are constant, making the PTG capacitance the sole variable influencing the capacitive current. The PTG capacitance of a line is proportional to its length and can be expressed as:

$$C_0 = c_0 \cdot l \tag{6}$$

Where l denotes the length of the line, and c_0 represents the capacitance per unit length of the line.

The capacitive current in a line is proportional to its length. Within a 10 kV system, if the capacitive current during a STG fault surpasses the 20 A threshold, a sustained grounding arc may develop. To mitigate this risk, the installation of an arc suppression coil at the neutral point is required, with the corresponding system configuration depicted in Fig. 2.

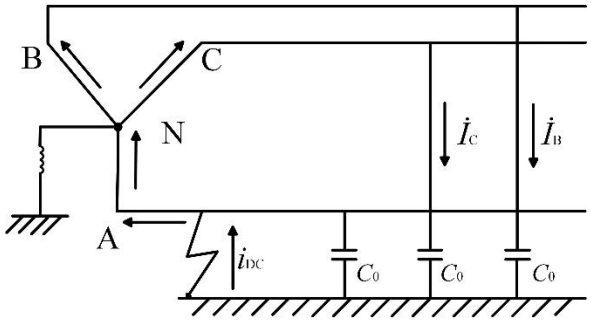

Fig. 2. Schematic of a small-current grounding system compensated by an arc suppression coil during a STG fault.

Following the installation of an arc suppression coil at the neutral point of the system:

$$\dot{I}_{DC} = \dot{I}_B + \dot{I}_C + \dot{I}_L \tag{7}$$

Where, the currents in phases B and C are capacitive, while the current through the arc suppression coil is inductive. The inductive current from the arc suppression

coil compensates for the capacitive current generated during the single-phase ground fault, thereby extinguishing the resulting arc.

2.2 Particle Swarm Optimization Strategy

The GA-PSO hybrid optimization strategy integrates both algorithms: the PSO is applied to automatically calibrate the parameters in the capacitive current model, while leveraging the GA's strengths to collectively boost search efficiency and escape local optima. The underlying principle is as follows:

The parameters to be optimized are defined as a three-dimensional decision vector:

$$x = [w_p, w_s, \gamma]^{\cdot} \tag{8}$$

Here, w_p is the weight coefficient of the public line, and w_s is the weight coefficient of the dedicated line, γ is an additional proportional coefficient for the substation, used to quantify the contribution of electrical equipment within the substation to the system's single-phase ground capacitance current.

The position $x_i(t)$ of each particle i at iteration t represents a set of candidate parameters. Its search space is defined by the physical constraints of each parameter:

$$x_{\min} \le x_i(t) \le x_{\max} \tag{9}$$

The PSO module [13] emulates swarm intelligence, wherein every particle's movement is guided by its personal best (pb) and the swarm's global best position. The velocity update for particle I in dimension d at the next iteration $v_{i,d}(t+1)$ is given by:

$$v_{i,d}(t+1) = \omega \cdot v_{i,d}(t) + a_1 r_1 \cdot (p_{best,i,d} - x_{i,d}(t)) + a_2 r_2 \cdot (g_{best,d} - x_{i,d}(t)) \tag{10}$$

Here, ω is the inertia weight, set to ω=0.7; a_1 and a_2 are acceleration coefficients, both assigned a value of 1.5; r_1 and r_2 are random variables following a uniform distribution U(0,1); $v_{i,d(t+1)}$ is the velocity of the i-th particle in the d-th dimension for the next iteration.

The updated velocity directly determines the particle's new position, as defined by the following equation:

$$x_{i,d}(t+1) = x_{i,d}(t) + v_{i,d}(t+1) \tag{11}$$

Here, $x_{i,d}(t)$ represents the position of the i-th particle in the d-th dimension at the t-th iteration.

To ensure solution feasibility, a projected boundary handling strategy is employed:

$$x_{i,d}(t+1) = \max(x_{\min,d}, \min(x_{i,d(t+1)}, x_{\max,d})) \tag{12}$$

Here, $x_{\min,d}$ enotes the lower limit of the d-th dimension, while $x_{\max,d}$ denotes its upper limit.

The velocity of particles exceeding the boundaries is set to zero or reversed to guide them back to the feasible search space.

2.3 Genetic Algorithm

The Genetic Algorithm enhances population diversity, introduces global exploration capabilities, and prevents premature convergence to local optima. In this model, each candidate solution is represented by a chromosome directly encoded by the decision variables to be optimized [14], where each variable possesses well-defined physical significance and boundary constraints:

$$x = [w_p, w_s, \gamma] \tag{13}$$

This module incorporates three classic genetic operators: selection, crossover, and mutation.

(a) Selection

The primary objective of the selection operation is to filter high-quality individuals from the current population and transfer them into the mating pool. This study adopts a hybrid selection mechanism combining the elitist strategy [15] and roulette wheel selection [16].

To prevent the loss of the best-performing solutions, an elite preservation strategy is employed, where the five fittest individuals from the current population are automatically transferred to the next generation. For the remaining individuals, a roulette wheel selection strategy based on the reciprocal of fitness is applied. In the minimization problem, the smaller the fitness value $F(x_i)$ of an individual x_i, the higher its probability $P(x_i)$ of being selected. The selection probability is calculated as follows:

$$P(x_i) = \frac{1/\left(F(x_i)\right)}{\sum_{j=1}^{N} 1/\left(F(x_j)\right)} \tag{14}$$

This strategy ensures that high-quality individuals have a greater chance of participating in reproduction, while retaining the possibility for low-quality individuals to contribute to diversity.

(b) Crossover

The crossover operation mimics the genetic recombination mechanism in biology and serves as the core operation for generating new individuals. This study employs an arithmetic crossover method [17]: for a pair of parent individuals p_1 and p_2 selected from the mating pool, whether crossover is performed is determined by a predefined crossover probability.

The random determination of a crossover point enables the linear combination of subsequent gene segments, resulting in two offspring: c_1 and c_2. This can be expressed mathematically as:

$$\begin{cases} c_1 = \alpha \cdot p_1 + (1-\alpha) \cdot p_2 \\ c_2 = \alpha \cdot p_2 + (1-\alpha) \cdot p_1 \end{cases} \tag{15}$$

where α is a random number uniformly distributed in the interval [0,1].

Arithmetic crossover enables a systematic search within the hyperplane defined by the parent individuals, thereby exhibiting strong local exploitation capabilities and contributing to improved convergence accuracy of the algorithm.

(c) Mutation

The mutation operation [18] randomly alters gene values with a small probability, simulating genetic mutations. It serves as a key mechanism for maintaining population diversity and facilitating global exploration. Gaussian mutation is adopted in this study.

For each individual, an identical mutation probability is set to determine whether mutation occurs.

If mutation is triggered, a randomly selected gene is perturbed by adding a Gaussian random disturbance [19] to its current value:

$$g' = g + N(0, \sigma) \tag{16}$$

Here, g represents the gene value before mutation, and g' represents the new gene value after the mutation operation. The standard deviation σ is set to 10% of the width of the corresponding parameter range for that gene. The mutated gene value is constrained within predefined boundaries to ensure the validity of the solution. The flowchart of the GA-PSO algorithm is shown in Fig. 3.

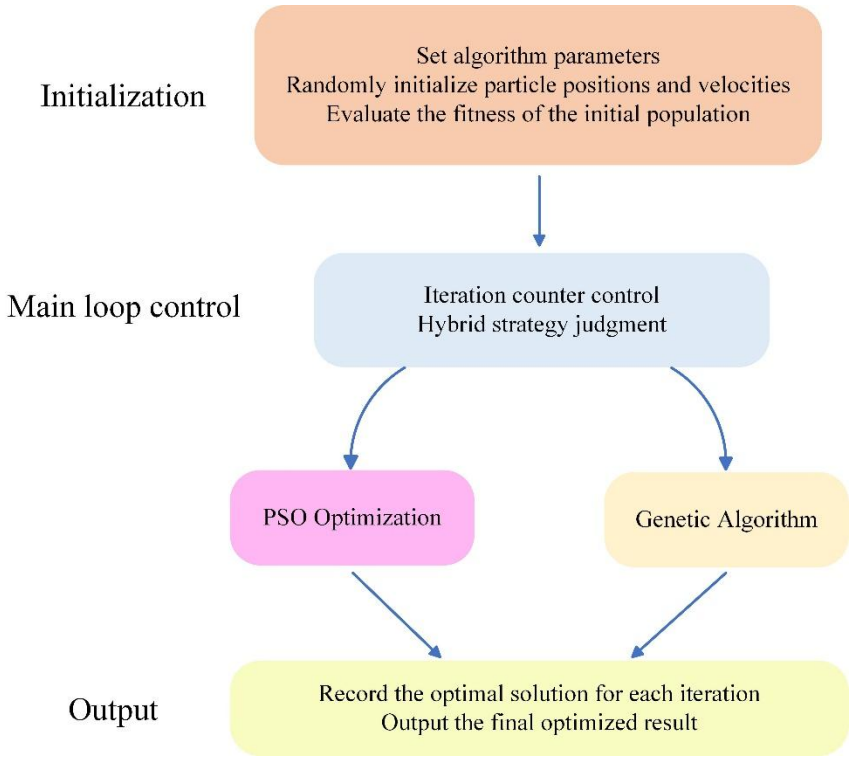

Fig. 3. Flowchart of the GA-PSO Algorithm.

2.4 Fitness Evaluation Function for Monte Carlo Simulation

In traditional optimization algorithms dealing with deterministic models, the fitness function is typically a deterministic calculation. However, the distribution network capacitive current calculation problem addressed in this paper involves significant uncertainties in the input parameters. To fundamentally address these uncertainties, this study embeds Monte Carlo Simulation (MCS) [20] into the fitness evaluation step of the optimization algorithm, constructing a probabilistic fitness evaluation function. This function generates the probability distribution of the capacitive current through Monte Carlo Simulation and uses the statistical characteristics of this distribution as the evaluation basis. The mathematical expression is as follows:

$$F = \sqrt{\frac{1}{\mathrm{N}} \sum_{i=1}^{\mathrm{N}} (I_i - \mu)^2} \tag{17}$$

Where N is the number of Monte Carlo simulations; I_i represents the total system capacitive current obtained from the i-th simulation; and μ denotes the mean value of the N simulation results.

In each Monte Carlo simulation, the capacitive current contribution of a single line is given by:

$$I_{ij} = \sum_{k=1}^{\mathrm{M}} \left[L_{jkpublic} \cdot U_{jk} \cdot w_{\mathrm{p}} \right] + \sum_{k=1}^{\mathrm{M}} \left[L_{jkprivate} \cdot U_{jk} \cdot w_{\mathrm{s}} \right] \tag{18}$$

Where M represents the number of conductor types included in the line; L_{jk} denotes the length of the k-th type of conductor; U_{jk} refers to the unit capacitive current of the k-th type of conductor; W_{jk} is the weighting coefficient, which comprises the public line weighting factor $\mathrm{w_p}$ and the dedicated line weighting factor $\mathrm{w_s}$.

The total capacitive current I_i of the system is given by:

$$I_i = \sum_{j=1}^{K} I_{ij}(1+\gamma) \tag{19}$$

Herein, K represents the total number of lines; γ denotes the additional proportional coefficient of the substation.

A smaller fitness value F indicates that the parameter set($\mathrm{w_p}$, $\mathrm{w_s}$, γ) better reduces the fluctuation in computational results, thereby enhancing the model's robustness and prediction accuracy. Through an iterative process, the parameters are refined to seek the minimization of F, leading to the optimal parameter set detailed in Table 1.

Table 1

Monte Carlo algorithm procedure

Single Monte Carlo Simulation
For each line:
(1) Determine the unit current range based on the line type.

(2) Randomly sample a unit current value from the range. (3) Calculate the weighted length. (4) Compute the line's capacitive current contribution.
Statistical Calculation
(1) Repeat the simulation N times. (2) Calculate the mean (μ) and standard deviation (σ). (3) Return σ as the fitness value.

3. Experimental Procedure

3.1 Experimental Processing

This experiment employed the following parameter settings: The PSO used a swarm of 30 particles and was run for 100 iterations. For the GA, the crossover and mutation probabilities were assigned values of 0.8 and 0.1, respectively, with an elite count of 5. The MCS was conducted with 1000 simulation samples. In the model, the value range of the public line weight is [0.9, 1.1], the dedicated line weight range is [1.0, 1.2], and the additional ratio range of the substation is [0.08, 0.15]. The software environment for the experiment was conducted on a platform running a 64-bit Windows 10 operating system, powered by an Intel i5-12600KF CPU and an NVIDIA GeForce RTX 4060 Ti GPU. The algorithms are implemented under the PyTorch 1.10.2 framework, and the programming language is Python 3.6.5.

The line dataset used in the experiment is derived from the 10kV distribution line (Yulong) parameter table provided by the Hohhot Power Supply Company in China, the specific parameters can be found in Fig. 4 and Table 2.

Table 2

Yulong Line Line Parameters

No.	Line type	Line name	Feeder cable type	OPL	ODL	CPL	CDL	TOC	ML	TL
1	HCOL	951	YJV22-10-3×300mm^2	0.00	0.75	0.00	8.98	0.75	9.73	9.73
2	HCOL	952	YJV22-10-3×300mm^2	0.00	0.75	0.00	8.98	0.75	9.73	9.73
3	ACL	953	YJV22-10-3×300mm^2	0.00	0.00	0.00	4.20	0.00	3.90	4.20
4	HCOL	955	YJV22-10-3×300mm^2	4.20	1.86	0.56	1.10	6.06	2.27	7.72
5	ACL	956	YJV22-10-3×300mm^2	0.00	0.00	0.00	6.30	0.00	5.10	6.30
6	HCOL	957	YJV22-10-3×240mm^2	5.23	0.00	3.16	0.81	5.23	7.61	9.20
7	HCOL	958	YJV22-10-3×240mm^2	1.10	0.00	2.84	0.00	1.10	1.53	3.94
8	HCOL	959	YJV22-10-3×300mm^2	4.73	0.35	0.20	1.50	5.08	3.63	6.78
9	HCOL	960	YJV22-10-3×300mm^2	4.40	1.10	2.60	7.40	5.50	4.40	15.50

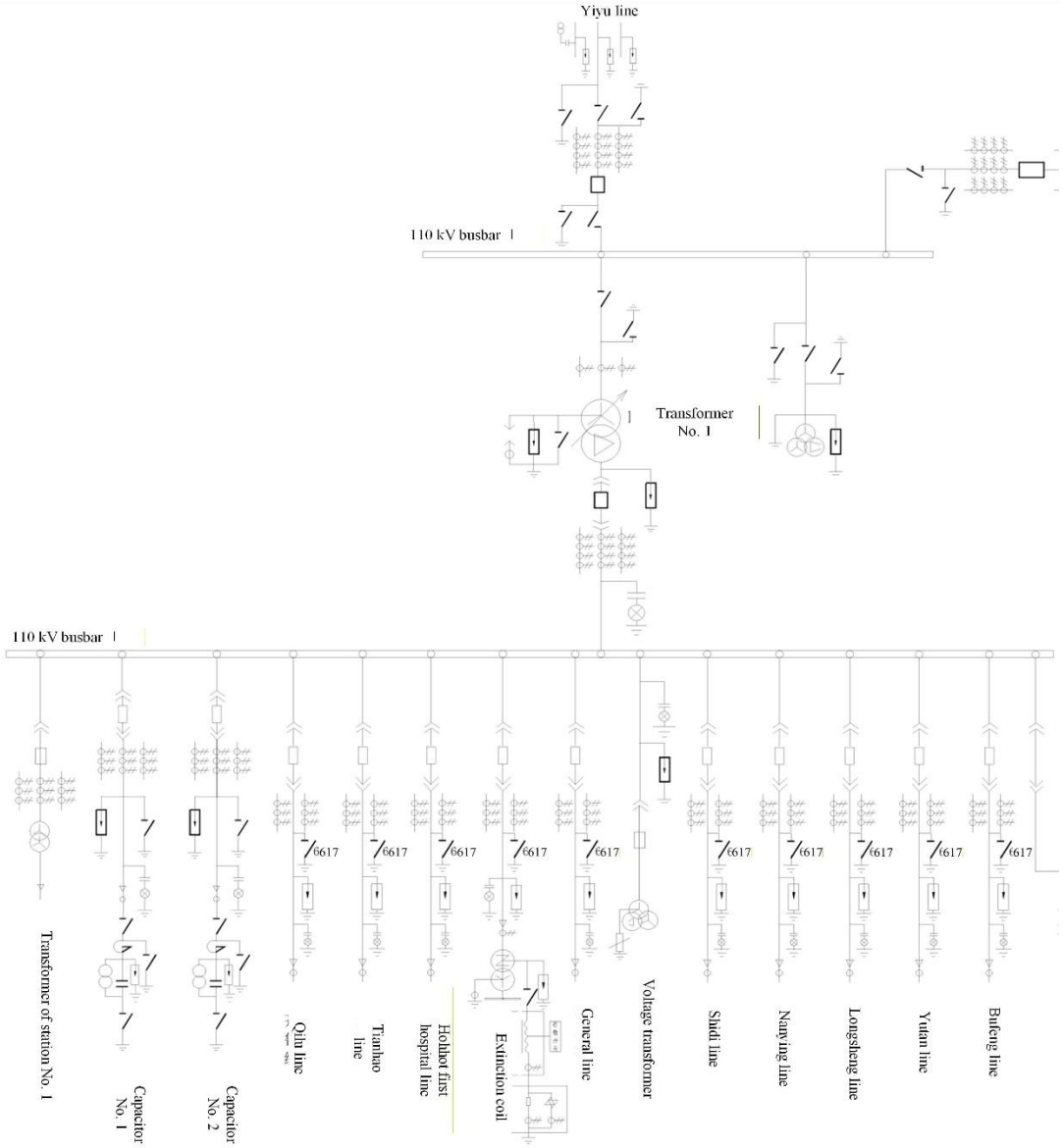

Fig. 4. Yulong line electrical wiring diagram.

This dataset includes fields such as line name, outlet cable type, main line conductor type, public overhead line length, dedicated overhead line length, dedicated cable length, dedicated insulated overhead line length, main line length, total line length, interconnection type, and line category. It fully covers all parameter information of the Yulong line, demonstrating good authenticity and representativeness.

In Table 2, HCOL stands for Hybrid cable-overhead line, ACL for All-Cable Line, OPL for Overhead length of public lines/km, ODL for Overhead length of dedicated lines/km, CPL for Cable length of public lines/km, CDL for Cable length of dedicated lines/km, TOC for Total length of overhead insulated conductors/km, ML for Main line length/km, and TL for Total line length/km.

To analyze the performance of the model proposed in this paper, the variation curve of the fitness value of the GA-PSO-MCS hybrid algorithm during the optimization process is plotted. In Fig. 5 (a), the red dashed line indicates the iteration times when GA operations (including selection, crossover, and mutation) are performed. In engineering calculations, the standard deviation is an important indicator for evaluating the fluctuation and reliability of results. A smaller value indicates a better parameter combination and lower prediction uncertainty. From Fig. 5 (b), it can be observed that the optimization process overall shows a downward trend, with significant decreases in the fitness value after the 5nd and 35th iterations, particularly showing clear improvement after the introduction of genetic operations; the algorithm finally converges and stabilizes after the 37th iteration, with the fitness value remaining around 1.25, indicating that the corresponding parameter combination has reached the optimum and the calculation results have low uncertainty.

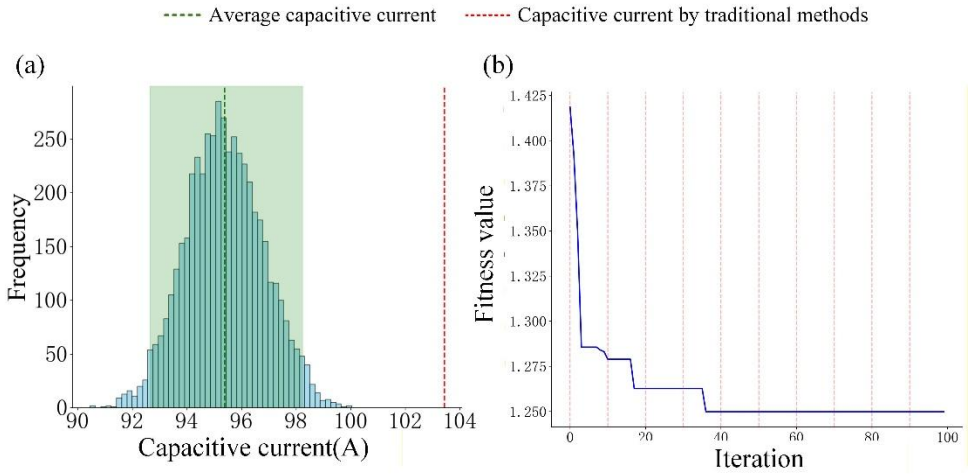

Fig. 5. GA-PSO-MCS (a) Capacitive Current Histogram, (b) Standard Deviation Variation Curve.

3.2 Experimental Comparison

This study proposes a hybrid GA-PSO algorithm. Its performance was evaluated against two established optimization techniques: the standard Particle Swarm Optimization (PSO) and Bayesian Optimization (BO). To ensure a fair comparison, the parameters of the standalone PSO algorithm were kept identical to those of the PSO module within the GA-PSO hybrid. For the BO algorithm, we set

the total number of evaluations to 100 and the number of initial random points to 10.

Fig. 6 (c) depicts the convergence trajectories of all three algorithms over 100 iterations. All methods exhibited a rapid decrease in the objective function value within the first 15–40 iterations before plateauing. BO converged most rapidly, reaching a value of 1.34 after only 15 iterations; however, it yielded the worst final solution among the three. Both PSO and GA-PSO converged later, at 37 iterations, to values of 1.27 and 1.25, respectively. Notably, GA-PSO achieved the best final performance. This result confirms that the integration of genetic algorithms' global exploration capability with the local exploitation strength of particle swarm optimization enables GA-PSO to find a superior solution while maintaining a convergence speed comparable to that of PSO.

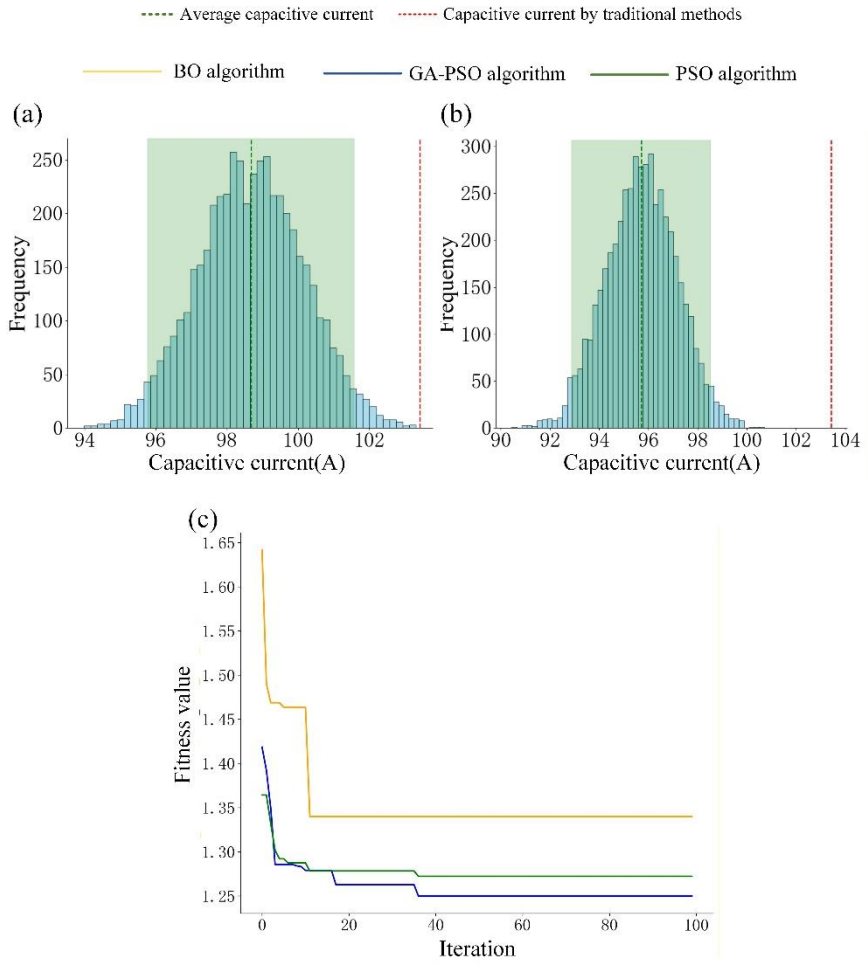

Fig. 6. (a) Capacitive current histogram of PSO-MCS, (b) Capacitive current histogram of BO-MCS, (c) Comparison chart of convergence of three methods

Table 3

Comparison of computational results without MCS algorithm

Parameter / Methods	Public line weight	Special line weight	Substation additional ratio	Average capacitive current/A	Standard deviation
Fixed parameter	1.0	1.05	0.1	103.42	
PSO	0.9	1	0.081	95.45	1.34
GA-PSO	0.9	1	0.08	95.55	1,32
BO	0.9	1	0.08	95.39	1.44

Based on the analysis of Table 3 and Fig. 6 (a),(b), it can be observed that when excluding the MCS module, among the four methods mentioned, the traditional method employs higher values for the public line weight, dedicated line weight, and substation additional ratio, compared to the other three optimization methods. The capacitive current value calculated by this method is also the largest, reaching 103.42 A. However, this method can only provide a single estimated value for the capacitive current, without the ability to further evaluate the uncertainty of the result, and it exhibits a significant overestimation phenomenon.

In contrast, after optimization by the algorithms, the parameter values of the PSO-MCS, GA-PSO-MCS, and BPT-MCS methods are significantly reduced and stabilize around a public line weight of 0.9, a dedicated line weight of 1.0, and a substation additional ratio of 0.08. Although the differences in the average capacitive current values obtained by the three optimization methods are small, the standard deviation of the GA-PSO-MCS method is significantly lower than those of PSO-MCS and BPT-MCS, at only 1.32 A, indicating that the results of its multiple Monte Carlo simulations are more concentrated and exhibit lower uncertainty. Thus, it can be concluded that GA-PSO-MCS effectively enhances the stability and reliability of the results while maintaining high computational accuracy.

Table 4

Comparison of computational results with MCS algorithm

Parameter / Methods	Average capacitive current/A	Confidence interval	Standard deviation	Difference
PSO-MCS	95.49	(92.63, 98.30)	1.44	7.7
GA-PSO-MCS	95.56	(92.78, 98.31)	1.43	7.6
BPT-MCS	95.37	(92.55, 98.14)	1.43	7.8

Following the completion of parameter optimization, a fair evaluation is conducted for all methods using an equal number of Monte Carlo simulations. This approach eliminates the influence of randomness inherent in the optimization process and directly compares the accuracy and reliability of the final results across different methods. As shown in Table 4, the standard deviations of the three methods are nearly identical, and the computational results of the optimized methods are close to those of the traditional fixed-parameter method. This indicates

that all three optimization methods perform excellently and comparably in terms of uncertainty control. Among them, GA-PSO-MCS yields the highest average capacitive current value. Additionally, the upper confidence limit of this method is 98.31 A, suggesting that the risk of the actual capacitive current calculated by GA-PSO-MCS exceeding the coil capacity during future system operation is the lowest.

4. Conclusions

The GA-PSO-MCS fusion algorithm proposed in this study effectively synthesizes the global search capability of GA and the rapid convergence of PSO, overcoming the tendency of single algorithms to be trapped in local optima. When combined with Monte Carlo Simulation's capacity for quantitative uncertainty description, this approach is systematically applied to capacitive current calculation in distribution networks. Analysis of computational results based on actual line parameters demonstrates that the proposed method not only significantly reduces estimation deviation and enhances robustness but, more critically, provides a highly reliable engineering basis for arc suppression coil selection by inherently supporting the fundamental over-compensation principle. By delivering probabilistic current distributions and confidence intervals rather than a single deterministic value, our approach enables the selection of coil capacity based on upper confidence bounds, thereby ensuring adequate over-compensation margins to prevent the risks of under-compensation and enhance system safety, demonstrating promising theoretical and practical outcomes in 10 kV distribution networks.

Acknowledgement

This research was funded by Science and Technology Project of Inner Mongolia Electric Power (Group) Co., Ltd.: Research and Application of Capacitive Current Monitoring and Arc Fire Mitigation Technologies in Medium-Voltage Distribution Networks (No. 2025-3-8).

R E F E R E N C E S

[1]. X. Ren, Y. Bai, Y. Dai, et al. “Research on the countermeasures of the single-phase-to-earth faults in flexibly grounded distribution networks”, in Alexandria Engineering Journal., **vol. 98**, July. 2024, pp. 68-79.

[2]. H. Wang, M. Guo, Z. Zheng, et al. “Suppression strategy on neutral point overvoltage in resonant grounding system considering single line-to-ground fault”, in Electric Power Systems Research., **vol. 6**, May. 2022, pp. 107782.

[3]. L. Jiang, X. Yin, X. Zeng, et al. “Flexible voltage arc suppression in distribution networks considering asymmetric ground parameters based on power router”, IEEE Transactions on Industrial Electronics., June. 2025, pp.1-12.

[4]. S. Shi, Q. Xie, P. Ma, et al. "A single-phase ground fault line selection method in active distribution networks based on transformer grounding mode modification", in Energies., **vol. 17**, Sept. 2024, pp. 4743.
[5]. L. He, L. Ge, B. Sun, et al. "Capacitive current measuring method for distribution networks based on resonant frequency prediction model", in Automation of Electric Power Systems., **vol. 42**, Janu. 2018, pp. 143-147.
[6]. Wu H, Sun Y, Liu X, et al. "The signal injection method with High-Frequency for distribution network capacitive current measurement", in Journal of Electrical Engineering and Technology., **vol. 16**, Feb. 2021, pp. 867-872.
[7]. C. Vlad and P. Monica. "Performance analysis of genetic algorithms for route computation applied to emergency vehicles in uncertain traffic", UPB Scientific Bulletin, Series C: Electrical Engineering and Computer Science, **vol. 82**, pp. 167-178.
[8]. Y. Yu, K. Lin, Y. Liu, et al. "PSO optimized SVM parameters for far infrared pedestrian detection", in UPB Scientific Bulletin, Series C: Electrical Engineering and Computer Science , **vol. 81**, pp. 15-26.
[9]. Y. Xiong, F. Liu and G. Liu. "Dynamic Bayesian network structure learning optimization algorithm based on BLDOO+CS", in UPB Scientific Bulletin, Series C: Electrical Engineering and Computer Science, **vol. 87**, pp. 261-274.
[10]. X. Su, H. Zhang, J. Zhang, et al. "Kernel-PCA-based single-phase earth fault detection model using multilayer perceptron in deep learning", in IET Generation, Transmission & Distribution., **vol. 18**, Jan, 2024, pp. 834-843.
[11]. O. Artur, G. Renê, B. André. "Learning decision variables in Many-Objective optimization problems", in IEEE Latin America Transactions., **vol. 21**, Sep. 2023, pp. 1157-1163.
[12]. S. Mahmoud. "Practical aspects of perimeter intrusion detection and nuisance suppression for distributed fiber-optic sensors", in IEEE Transactions on Instrumentation and Measurement., **vol. 72**, Jun, 2023 pp. 1-11.
[13]. R. Mohamed, E. Saber, S. Ruhul, et al. "Neuro-PSO algorithm for large-scale dynamic optimization", in Swarm and Evolutionary Computation., **vol. 94**, Apr. 2025, pp. 101865.
[14]. Y. Li, X. Huang, C. Zhao, et al. "A novel remaining useful life prediction method based on multi-support vector regression fusion and adaptive weight updating", in ISA Transactions., **vol. 131**, Dec 2022, pp. 444-459.
[15]. S. Duman. "A modified moth swarm algorithm based on an arithmetic crossover for constrained optimization and optimal power flow problems", in IEEE Access., **vol. 6**, Jun. 2018, pp. 45394-45416.
[16]. U. Deniz, S. Serap, A. Nurdan. "Developing a secure image encryption technique using a novel S-box constructed through real-coded genetic algorithm's crossover and mutation operators", Expert Systems with Applications., **vol. 256**, Dec 2024, pp. 124904.
[17]. Q. Zhao, V. Hautamäki, I. Kärkkäinen, et al. "Random swap EM algorithm for Gaussian mixture models", in Pattern Recognition Letters., **vol. 33**, Dec 2012, pp. 2120-2126.
[18]. Z. Cui, Y. Jin, Z. Zhang, et al. "An interval multi-objective optimization algorithm based on elite genetic strategy", in Information Sciences., **vol. 648**, Nov. 2023, pp. 119533.
[19]. A. Naskar, S. Ghosh, M. Kundu, et al. "Feature selection using guided population based genetic algorithm with modified crossover and parent selection", in Applied Soft Computing., **vol. 172**, pp. 112872.
[20]. H. Sun, Y. Qiu, J. Li, et al. "A method to reduce the sampling variability of time-domain fatigue life by optimizing parameters in Monte Carlo simulations", in Probabilistic Engineering Mechanics., **vol. 75**, Jan. 2024, pp. 103591.